Hindawi
Journal of Nanomaterials
Volume 2023, Article ID 9817636, 1 page
https://doi.org/10.1155/2023/9817636

Retraction

Retracted: Tribological Behavior and Surface Characterization of Gray Cast Iron-EN31 Steel under Lubricated Sliding Conditions

Journal of Nanomaterials

Received 11 July 2023; Accepted 11 July 2023; Published 12 July 2023

This article has been retracted by Hindawi following an investigation undertaken by the publisher [1]. This investigation has uncovered evidence of one or more of the following indicators of systematic manipulation of the publication process:

(1) Discrepancies in scope
(2) Discrepancies in the description of the research reported
(3) Discrepancies between the availability of data and the research described
(4) Inappropriate citations
(5) Incoherent, meaningless and/or irrelevant content included in the article
(6) Peer-review manipulation

The presence of these indicators undermines our confidence in the integrity of the article's content and we cannot, therefore, vouch for its reliability. Please note that this notice is intended solely to alert readers that the content of this article is unreliable. We have not investigated whether authors were aware of or involved in the systematic manipulation of the publication process.

Wiley and Hindawi regrets that the usual quality checks did not identify these issues before publication and have since put additional measures in place to safeguard research integrity.

We wish to credit our own Research Integrity and Research Publishing teams and anonymous and named external researchers and research integrity experts for contributing to this investigation.

The corresponding author, as the representative of all authors, has been given the opportunity to register their agreement or disagreement to this retraction. We have kept a record of any response received.

References

[1] S. Ananth, P. Sivaprakasam, J. Udaya Prakash, P. Maheandera Prabu, V. Perumal, and G. Kalusuraman, "Tribological Behavior and Surface Characterization of Gray Cast Iron-EN31 Steel under Lubricated Sliding Conditions," *Journal of Nanomaterials*, vol. 2021, Article ID 7725959, 9 pages, 2021.

Hindawi
Journal of Nanomaterials
Volume 2021, Article ID 7725959, 9 pages
https://doi.org/10.1155/2021/7725959

Research Article

Tribological Behavior and Surface Characterization of Gray Cast Iron-EN31 Steel under Lubricated Sliding Conditions

S. Ananth[1], **P. Sivaprakasam**[2], **J. Udaya Prakash**[3], **P. Maheandera Prabu**[4], **Varatharaju Perumal**[5] and **G. Kalusuraman**[6]

[1]*Department of Mechanical Engineering, Shri Ram Murti Smarak College of Engineering & Technology, Bareilly, India*
[2]*Department of Mechanical Engineering, Center of Excellence-Nano Technology, College of Electrical and Mechanical Engineering, Addis Ababa Science and Technology University, Addis Ababa, Ethiopia*
[3]*Department of Mechanical Engineering, Vel Tech Rangarajan Dr. Sagunthala R&D Institute of Science and Technology, Chennai, India*
[4]*Department of Ocean Engineering, Indian Institute of Technology Madras, Chennai, Tamil Nadu, India*
[5]*Department of Automotive Technology, Ethiopian Technical University, Addis Ababa, Ethiopia*
[6]*Department of Agricultural Engineering, Kalasalingam Academy of Research and Education, Krishnankoil, Tamil Nadu, India*

Correspondence should be addressed to P. Sivaprakasam; shiva@aastu.edu.et

Received 10 July 2021; Accepted 28 September 2021; Published 14 October 2021

Academic Editor: Karthikeyan Sathasivam

This research investigates the tribological behavior of gray cast iron against EN31 steel under lubricated conditions. The most typical lubricated sliding phenomena are the reduction of wear on both the sliding surfaces and any one of the critical surfaces. Static and hydrodynamic wear can be reduced based on fluid properties or the accessibility of fluid between the surfaces. The oil's viscosity or content of the hydrocarbon and additives present in the oil plays a major role in controlling the wear of reciprocating surfaces. Therefore, this research work focused on metal-to-metal contact wear under the influence of lubricating oil (40 pride oil). The Taguchi method was used to select the sliding parameter combinations. Lubricated sliding resulted in a relatively reduced order of friction coefficient, attributable to better load distribution due to the formation of the lubricant film.

1. Introduction

Gray cast iron (GCI), used in the manufacturing of industrial components, is more accessible to machines and requires less lubricant than other cast irons [1]. This study deals with the sliding wear behavior of GCI-steel (EN31) contact pair under lubricated conditions over a range of load, sliding speed, and sliding distance. A solid-solid contact/solid-fluid contact pair is the most common type of contact pair. Solid-solid contact could be expected corrosion, adhesion, abrasion, and diffusion wear [2]. Tribological characteristics such as friction and adhesion wear are considered in the current study of solid-solid contact. GCI exhibits the essential microstructure and is commonly used in wear-resistant products such as cylinder liners, piston rings, clutches, and disc brakes [3].

Prasad [4] examined the sliding wear behavior of GCI in dry and lubricated conditions (SAE 40) over a range of sliding speeds and pressure. It was found that the cast iron wear rate increased with sliding speed and applied pressure. The temperature increased initially at a high rate in the specimen's surface after reducing the later stages of sliding at low pressures. Adhesion plays a significant role in causing oil and oil content loss plus graphite-lubricated state. Oil wear rate is lower than dry wear rate [4]. Grabon et al. [5] measured the tribological quality of honed cylinder liners made from GCI on the plateau. The selected counterpart material consisted of piston rings of GCI.

A reciprocating test was used for comparing the honed cylinder liner with or without additional oil pockets (SAE 40 diesel engine oil) created by the burnishing method. In addition, dimples were prepared on the surface of the honed

cylinder liner, which shows a reduction of half of the friction coefficient as in the usual surface. Each grade of industrial lubricant usually comes with several additives that are physically or chemically absorbed on the surface to avoid aggressive wear conditions under the boundary lubrication regime. Lubricants are primarily used to separate two sliding surfaces to reduce friction and wear. It also serves other purposes, including removing heat and pollutants from the contact. Lubricants are typically made up of oil plus compounds called additives that assist oils in performing specific roles successfully [6].

Flake Graphite Iron (FGI) is highly suggested for wear resistance applications among the GCI due to its flaky graphite structure [7]. GCI is generally used in automotive applications, particularly cylinder liners. According to the literature, the best wear-resistant microstructure is a pearlitic matrix with a tiny quantity of free ferrite. GCI includes such a matrix, and its use for a range of tribological applications has been seen in the past, particularly in sliding contact systems [8, 9].

The wear map for ASTM A30 GCI was created with a pearlitic matrix, which summarized the wear rate and its mechanisms into ultramild, mild, and severe wear regimes by Riahi and Alpas [10]. There was no palpable evidence of plastic deformation in ultra and mild wear formation of oxide layers covering contacting surfaces. The material was transferred on the surface of the AISI 52100 steel as a counter face because surface roughness increased from 0.12 μm to 4.0 μm. The hardness, temperature, and surface roughness increased during the severe wear regime due to surface deformation on the cast iron and welded on the EN31 steel with a maximum height of 10 μm. The severe wear appeared when oxide layer formation was unstable due to delaminating of tribe oxides. The author has referred to the formation of graphite flakes under low loading conditions during dry sliding which reveals excellent wear resistance of GCI [10].

The wear behavior of different compositions of alloyed gray cast iron tested against hardened steel (62 HRC) was analyzed [11]. The results show that the alloyed hypereutectic cast iron has three times lower wear rate than the elemental iron, owing to the larger graphite content and strong carbides in the matrix. Also, tensile strength and specific wear rate decrease with increasing graphite volume. Simultaneously, due to three-body abrasion, the hard carbide particle present in debris generation started along the wear track, preventing material loss during sliding. Chawla et al. [12] investigated the GCI wear mechanism, using the pin-on-disc wear tests under dry sliding conditions. The results show greater wear in stainless steel 304 with an increase in sliding speed at normal load and getting softened with an increase in the load parameter. But the wear ratio of GCI has been low with increasing load due to graphite (ferrite) matrix and decohesion observed. Masuda et al. [13] conducted sliding wear experiments under lubrication using gray cast iron AISI NO.35B. Wear surface and sliding wear mechanism was observed during the sliding wear process. The aluminium-modified cast iron (Fe-C-Al) has lower wear resistance and friction when compared to conventional (Fe-C-Si) cast iron [14]. Singh and Bhowmick [15] investigated the tribological behavior of hybrid AMMC sliding against steel and cast iron with MWCNT-oil lubrication; the inclusion of lubricants permits the creation of tribo layers which controls the relevant antifriction and antiwear processes.

Prasad [16] investigated the wear characteristics of GCI in both dry and oil-lubricated environments. It was found that the wear rate of cast iron increased with the sliding speed and pressure. At the initial stage due to adhesion, the temperature near the specimen surface increased, whereas at later stages the temperature decreased at low pressure. In practice, GCI-steel contact pair finds wide application. The base GCI has superior mechanical properties like good vibration damping, low coefficient of friction, good toughness, and excellent wear resistance. Gray cast iron type consists of predominantly pearlitic/ferrite matrix or both with graphite flakes. Even though it has good properties, it must withstand the application environments such as dry and lubricated sliding, which has exposed positive and negative wear. Many researches attempted wear behavior of gray cast iron under wet conditions, but limited studies reported on positive and negative behavior of GCI. Therefore, this research describes the lubricated environment conditions under the contact pair of GCI-EN31 steel.

Table 1: Chemical composition of grade GCI specimen (BS 1452).

Material	C	Si	Mn	S	Cr	P	Cu	Fe
Weight%	3.2	2.1	0.7	0.06	0.3	0.25	1.5	Remainder

Table 2: Process parameter and their levels.

Levels	Parameters		
	Load (N)	Sliding speed (m/s)	Sliding distance (m)
1	15	0.5	300
2	30	1.0	600
3	45	1.5	900

2. Experimental Procedure

2.1. Selection of Material. Cast iron (200-250/BS 1452, also called GCI) is a popular material used in modern industrial applications. The price is so low (20-40%) than the steel, and it has a wide variety of mechanical properties. High carbon and chromium-containing low alloy steel EN31 (AISI 52100) was selected as a counter face specimen for this experiment. The chemical composition of GCI is tabulated in Table 1.

2.2. Test Parameters. Table 2 shows the wear test parameters such as load, sliding speed, and sliding distance. Wear study was carried out under dry and lubricated (40 pride oil) conditions using pin-on-disc tester shown in Figure 1. A combination of test parameters was selected and experimented based on the Taguchi design of experiments (DOE) principle with orthogonal array (OA) of L_{27}. The contact surface comprises stationary pins made of EN31 steel against a rotating

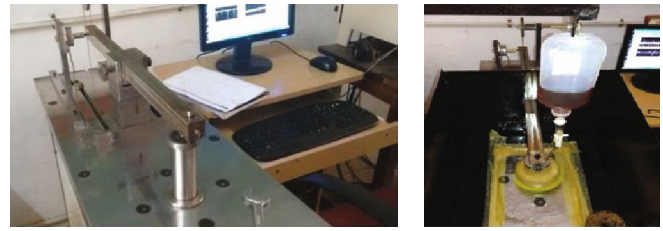

(a) Dry conditions (b) Lubricated conditions

Figure 1: Photograph of pin-on-disc wear tester.

Table 3: Experimental results.

S. no.	Load (N)	Sliding speed (m/s)	Sliding distance (m)	COF	Disc wt. loss (g)	Pin wt. loss (g)
1	15	0.5	300	0.1066	0.0028	0.052
2	15	0.5	600	0.0847	-0.0018	0.009
3	15	0.5	900	0.1146	-0.008	-0.006
4	15	1.0	300	0.0808	0.0041	0.006
5	15	1.0	600	0.0973	-0.0058	0.009
6	15	1.0	900	0.1081	-0.0012	0.016
7	15	1.5	300	0.1084	0.0012	-0.001
8	15	1.5	600	0.0901	-0.0018	-0.009
9	15	1.5	900	0.0901	-0.0037	-0.021
10	30	0.5	300	0.124	-0.007	-0.004
11	30	0.5	600	0.1034	-0.0011	-0.016
12	30	0.5	900	0.1095	-0.002	-0.003
13	30	1.0	300	0.1258	0.0004	-0.002
14	30	1.0	600	0.1258	0.003	0.001
15	30	1.0	900	0.0902	0.001	-0.002
16	30	1.5	300	0.1167	-0.0005	-0.024
17	30	1.5	600	0.1033	0.0013	-0.003
18	30	1.5	900	0.1313	0.0021	0.004
19	45	0.5	300	0.1443	-0.0003	0.017
20	45	0.5	600	0.1257	-0.0002	-0.019
21	45	0.5	900	0.1262	0.0005	0.022
22	45	1.0	300	0.1227	-0.0004	-0.005
23	45	1.0	600	0.0948	-0.0014	-0.001
24	45	1.0	900	0.0976	0.0031	-0.083
25	45	1.5	300	0.0861	0.0037	-0.011
26	45	1.5	600	0.1125	-0.0028	0.001
27	45	1.5	900	0.11	0.0004	0.005

cast-iron disc under the standard testing condition of ASTM G99 [17–19]. The test conditions are chosen based on the literature review and experience gained through earlier tests.

2.3. Sample Preparation. GCI discs of outer diameter 55 mm, inner diameter 6 mm, and 10 mm thickness were machined to conduct the experiments. The surface hardness of GCI is 28 HRC.

The counter specimen pin EN31 was machined from BS 970 grade with 6 mm diameter and length 60 mm and hardened to 58 to 60 HRC.

3. Results and Discussion

3.1. Observation on Lubricated Sliding. The GCI disc and pin are examined with 40 pride oils (additive oil), and the results are tabulated in Table 3. Sliding wear tests were conducted under a lubricated environment using 40 pride oil. It is seen that the wear of GCI on the counter pin varies only marginally with 40 pride oil during sliding; it could be because additive oil does not affect low load and speed conditions. Figure 2(a) illustrates the variation of wear with increasing sliding speed under the load of 15 N for the GCI disc with various sliding distance. Figure 2(b) shows the variation of

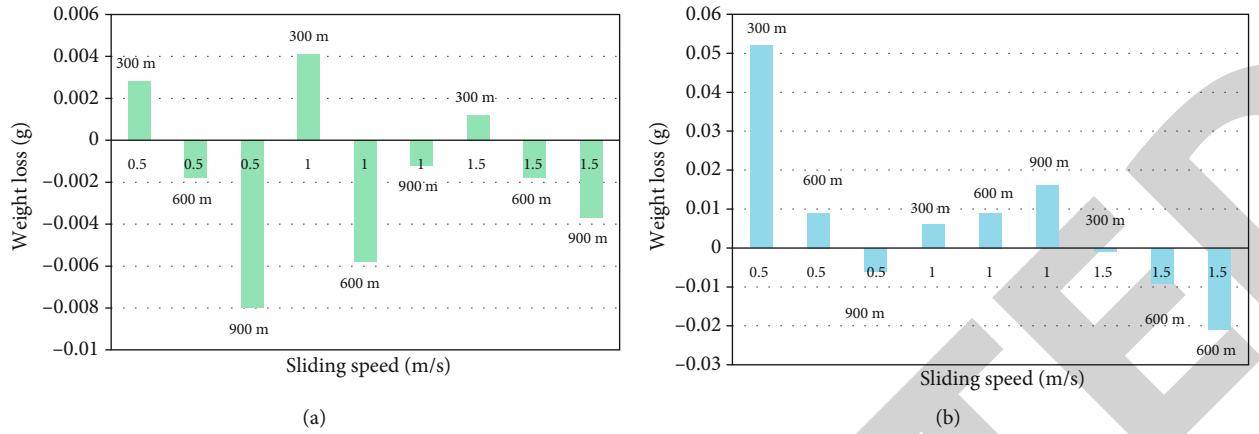

Figure 2: (a) Disc weight loss at 15 N load. (b) Pin weight loss at 15 N load.

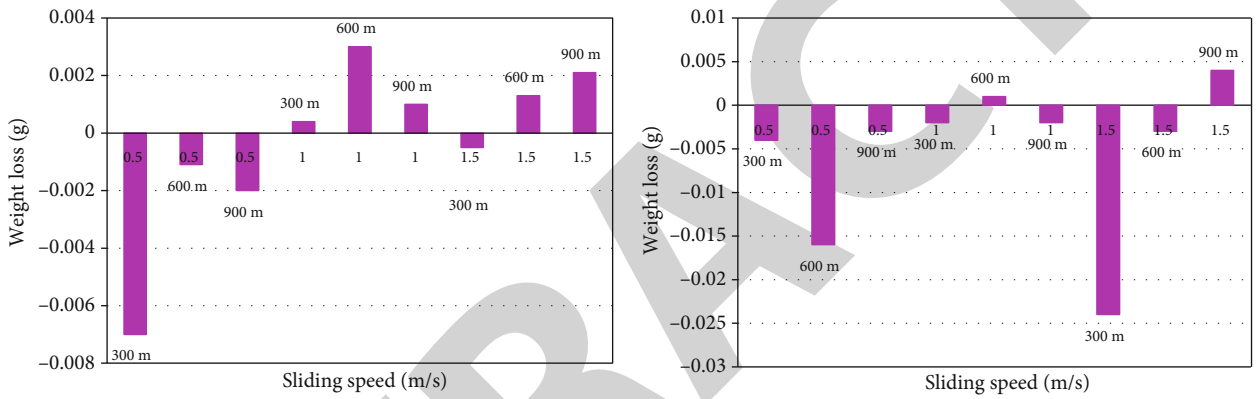

Figure 3: (a) Disc weight loss at 30 N load. (b) Pin weight loss at 30 N load.

wear with increasing sliding rate under the load of 15 N for EN31 steel pin with lubricated condition (40 pride oil).

From Figure 2(a), at 15 N load, it is seen that with 40 pride oil, the disc exhibits smaller order of wear and predominantly negative mode. With a lower speed of 0.5 m/s, sliding wear tends to drop down from positive to negative mode with the sliding distance. The change of wear mode could be attributed to the presence of transferred wear debris from the counter surface.

With increasing sliding speed (1 m/s), the disc encounters positive to negative mode of wear (marginally varying magnitude). With the higher speed of 1.5 m/s, an overall reduction in wear can be seen; the mode of wear changes from positive to negative mode. Typically monitored variation of wear of counter steel surface is illustrated in Figure 2(b). It is seen that with increasing speed and sliding distance, a gradual reduction in wear changing from positive to negative mode occurs. Sliding under 15 N load with a sliding speed of 1 m/s is seen.

At the same time, the counter steel surface exhibits a marginally increasing positive mode of wear; the GCI disc shows a fluctuating mode of wear, i.e., unlike the case of dry sliding. With 40 pride oil, under increasing speed (associated interface/contact temperature), likely, oil film factor on steel surface attributes to the reduction in wear; also, the occurrence of negative mode on both the contact surfaces could be due to effective transport of material between contact surfaces by the lubricant.

Figure 3(a) illustrates the variation of wear with increasing sliding speed under the load of 30 N for GCI disc. Figure 3(b) illustrates the variation of wear with increasing sliding rate under the load of 30 N for EN31 steel pin, in lubricated condition (40 pride oil). From Figure 3(a), GCI exhibits native wear at low sliding speed, whereas in increasing speed, it tends to rise to positive mode. The counter steel pin materials exhibit mostly negative wear. However, compared to 15 N loading, the counter steel pin surface exhibits a mainly negative mode of wear of relatively smaller magnitude. Also, it is seen that around 1 m/s sliding speed, a trend change can be observed. A similar observation is found, when wear losses increase as wear time, rotating speed, and applied pressure increase [20].

Figure 4(a) illustrates the variation of wear with increasing sliding speed under the load of 45 N for the GCI disc. Figure 4(b) shows the variation of wear with increasing sliding speed under the load of 45 N for EN31 steel pin, in lubricated condition (40 pride oil).

Unlike in the case of 15 N load (sliding), GCI disc exhibits mostly reduced order of wear; as observed in the trials, with this test condition (45 N), CI exhibits a visible rise

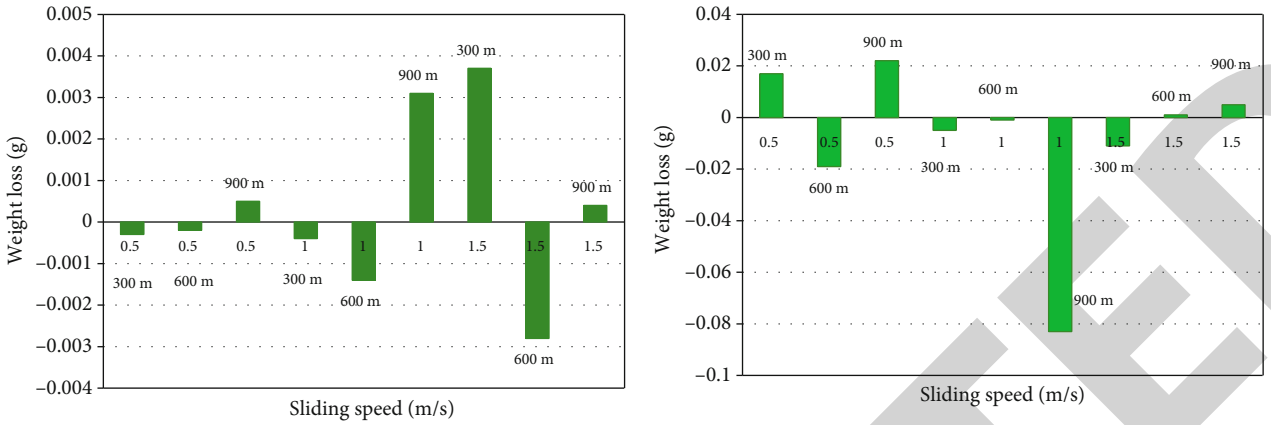

Figure 4: (a) Disc weight loss at 45 N load. (b) Pin weight loss at 45 N load.

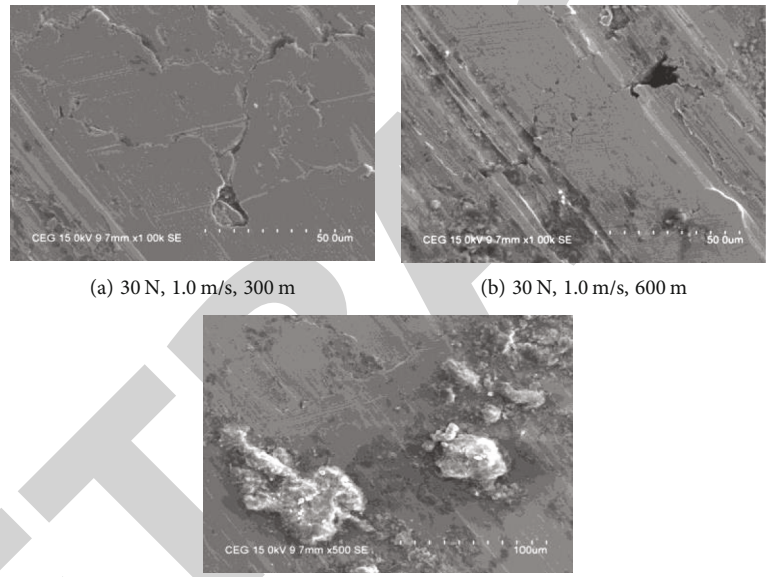

Figure 5: (a–c) Micrograph with 40 pride oil.

in wear (from -0.0014 to 0.0031 gms) at a sliding speed of 1 m/s and sliding distance of 900 m, thus indicating the dependency of adhesion wears on the PVT factor. Applied pressure may have the opposite effect by causing induced surface hardening, which in turn improves wear resistance [20].

Also, it is seen that a drop in adhesion wear can be seen with a higher speed of 1.5 m/s. This could be attributed to better film formation of this additive oil with increasing speed. Under the lubricated condition, it is known that the thickness of the lubricating film "h" is given in

$$h\,\alpha\,(\eta\,u)^{1/2}, \tag{1}$$

where η is the kinematic viscosity and u is the sliding velocity.

It is also known that when the film thickness exceeds the composite surface roughness of contacting surface, the Dowson ratio is calculated by using

$$D = \frac{h}{(V_{a1} + V_{a2})}\ (\text{Dowson ratio}). \tag{2}$$

V_{a1} is the roughness of CI; V_{a2} is the roughness of steel pin.

When "D" ratio is greater than 1-1.4, there will be effective separation of contacting surfaces, resulting in less interaction and wear.

Typical monitored variation of wear of counter steel surface at 45 N normal load is illustrated in Figure 4(b); with a lower sliding speed of 0.5 m/s, the pin exhibits relatively higher wear (0.017 mg-0.022 mg); with increasing sliding speed, 1 to 1.5 m/s, a reduction in wear (mostly negative mode) can be seen. With increasing sliding speed, better film formation results in enhanced wetting/absorption, causing a reduction in wear with the lower speed of 0.5 m/s, associated

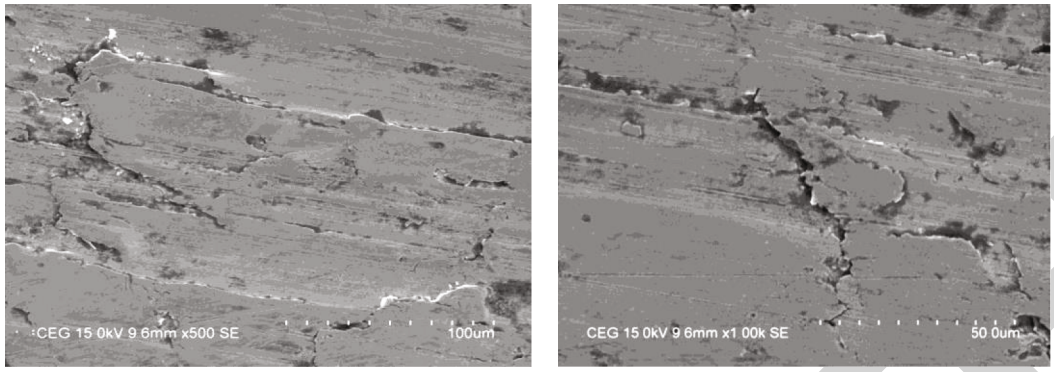

(a) 15 N, 0.5 m/s, 300 m (b) 15 N, 1.0 m/s, 300 m

Figure 6: (a, b) Micrograph with 40 pride oil sliding.

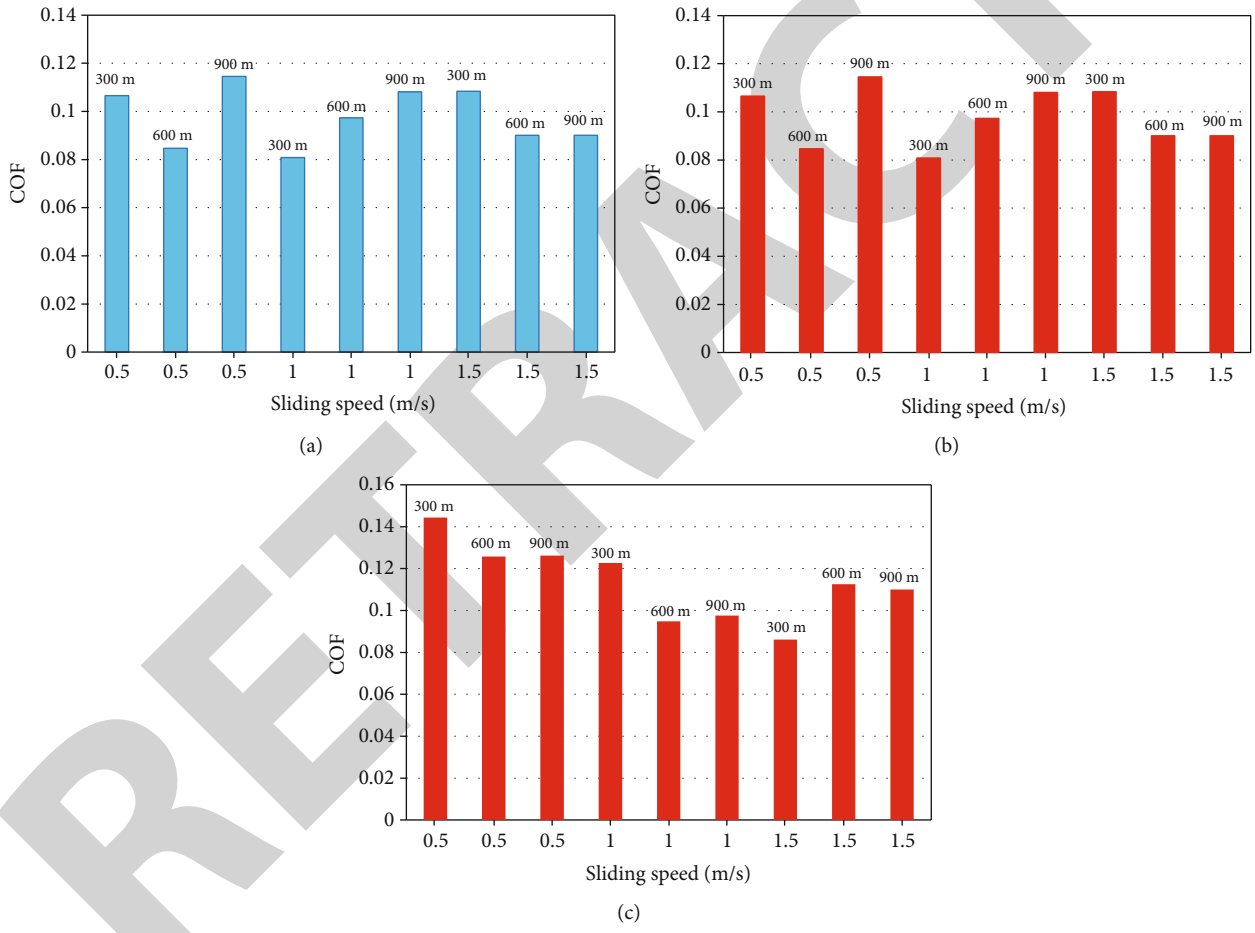

Figure 7: (a) COF at 15 N load. (b) COF at 30 N load. (c) COF at 45 N load.

with inadequate film formation, effectively a dry contact occurs, tending to enhanced wear. The observed higher order wear negative wear with 1 m/s sliding speed and sliding distance of 900 m could be attributed to the enhanced wear of GCI disc (at the same condition) and transfer.

3.2. Micrograph of Lubricated Sliding Conditions. A micrograph of worn-out sliding track on CI disc tested with 40 pride oil is shown in Figure 5(a). The positive mode of wear is associated with a worn-out micrograph showing surface cracking and discrete pits at the crack tip. Micrograph of worn-out surface on the sliding track of GCI disc presents partially glazed texture with discrete pull out of material shown in Figure 5(b). A typical micrograph in Figure 5(c) shows partially glazed texture, with discrete spots of transferred debris from the counter steel surface.

A micrograph of worn-out sliding track on GCI disc exposed to sliding contact with steel surface is shown in

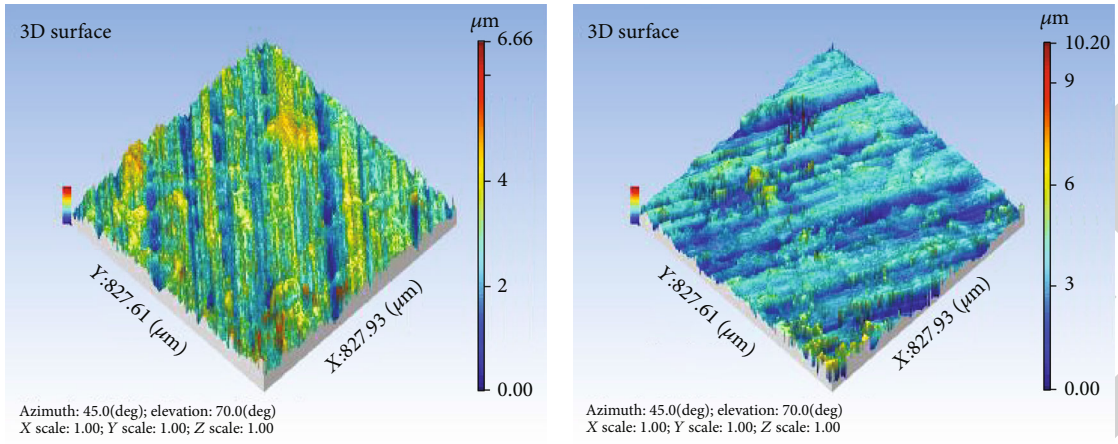

(a) 15 N, 0.5 m/s, 300 m (b) 15 N, 1.5 m/s, 300 m

Figure 8: (a, b) 3D surface texture views.

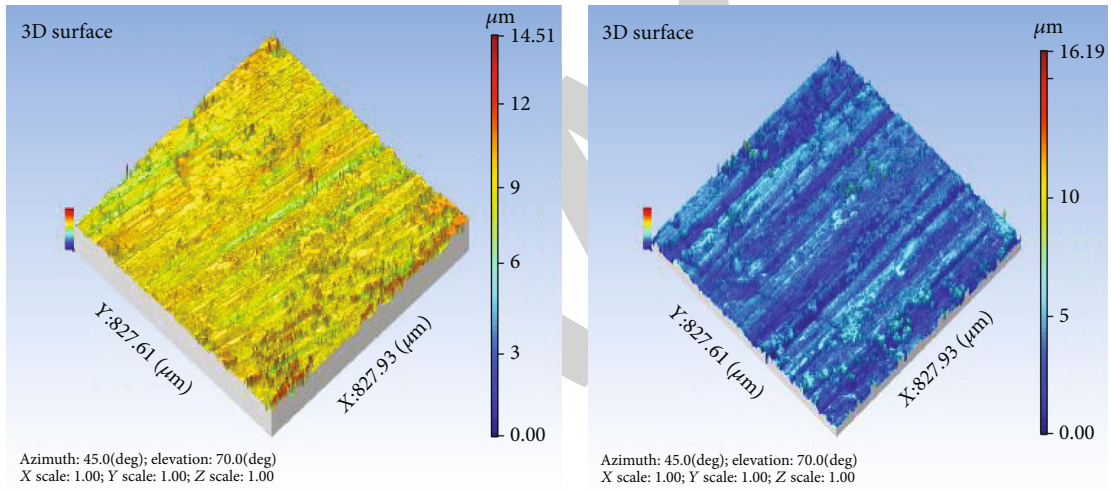

(a) 30 N, 1.0 m/s, 300 m (b) 30 N, 1.0 m/s, 900 m

Figure 9: (a, b) 3D surface texture views.

Figure 6(a) at 15 N load, 0.5 m/s, and 300 m. As presented earlier, the GCI disc encountered positive mode of wear, supplemented by the surface distress exhibited by the micrograph. Severe ridging and spalling of graphite can be seen. With additive oil such as 40 pride oil, under the low sliding condition of 15 N, 1.0 m/s, and 300 m, the contact would be dominating stick-slip in nature. The micrograph of worn-out track shown in Figure 6(b) pertains to a region of the track, exhibiting severe sliding spalling of graphite and discrete dents on the surface.

3.3. COF under Lubricated Contact. From Figure 7(a), the lower-order COF can be seen, with increasing load (30 N). COF marginally rises and is fluctuating around 0.1 to 0.123 with a higher load (45 N); a steady reduction in COF can be seen. The COF decreases and increases marginally with increased speed, indicating a slow improvement in wetting by the oil. The decrease part may be attributable to the wear of oxide film. At higher speeds, an almost steady state of COF occurs due to better film formation.

From Figure 7(b), the COF variation with increasing speed for 40 pride oil at 30 N load is very similar to 40 pride oil at 15 N. However, at most speeds, the COF value is marginally higher, which is attributable to higher load and lubricant inaccessible on the surface. It is seen that while the COF tends to rise with one m/s parametric combination, at 15 N, it tends to drop down for 45 N loading shown in Figure 7(c). This could be attributed to the increased surface interaction due to the accessibility of the additive oil to lubricate the interface at a low load. With increasing load, i.e., 45 N, possibly due to increasing contact temperature, better (lubricant) film formation occurs, tending to a reduction in COF.

3.4. 3D Surface Textures. Figure 8(a) shows the 3D surface texture which contains discontinuous sliding track/texture with transferred wear debris. A typical recorded surface profile is shown in Figure 8(a) and the following features: Ra −0.415 μm, Rt 3.77 μm, and Rz 2.72 μm relatively higher order Rt/Ra ratio (≈9); associated with a wavy texture,

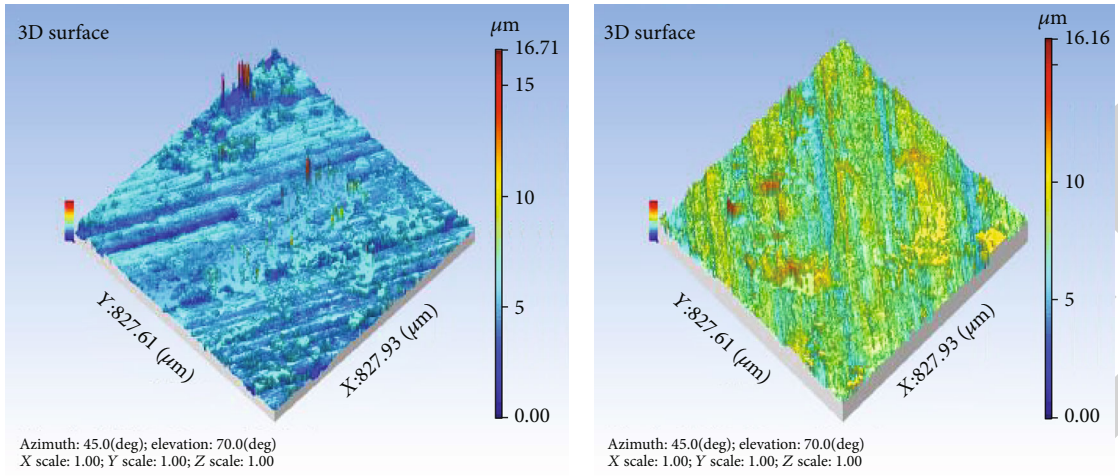

(a) 45 N, 0.5 m/s, 900 m (b) 45 N, 1.5 m/s, 900 m

Figure 10: (a, b) 3D surface texture views.

maximum peak height Rp 1.42 μm and maximum valley depth Rv −1.29 μm.

Under the severe test condition, relatively smoother texture observed is illustrated in Figure 8(b), higher speed, absence of stick-slip contact, hence resulting in the less wavy profile, with reduced Rt/Ra ratio Ra −0.386 μm, Rt −1.87 μm (Rt/Ra ≈ 5), Rp −0.746 μm, and Rv −1.03 μm. Reduction of Rp and Rv indicates mild crest flattening due to sliding. Kurtosis of 3.13 (typically 3) displaying reasonably uniform texture, also supplemented by the minor order skewness (Figure 8(b)), shows better texture Ra −0.386, Rv −1.87,Rt/Ra ≈ 5, kurtosis 3.17, and skewness 3.34 (left center texture).

Figure 9(a) presents a relatively smoother texture of distributed layer under medium load conditions (30 N, 1 m/s, 300 m) in mostly positive mode of wear. Profile indicates mild wavy texture, Ra −0.236 μm, Rt 1.9, andRt/Ra ≈ 8. The kurtosis (4.68) indicates wavy texture, skewness 0.266 left centric (nonuniform). In Figure 9(b), the 3D surface shows uniform texture with ridges, locally distributed lay Ra 0.18 μm, Rt 3.07 μm, and Rt/Ra > 10. The kurtosis is 3.18 and skewness is 0.224, wavy texture left centric (nonuniform texture).

Figure 10(a) depicts the surface texture feats of the worn-out track surface exposed to 45 N, 0.5 m/s, 900 m. The mild positive wear 3D texture, distributed pattern, locally crumbled surface and surface profile is right centric, Ra −0.682 μm, Rt 5.97, andRt/Ra ≈ 8. The kurtosis is 10.3 and skewness is 0.37. Wavy texture is presented (due to crumbling of material). In another region from Figure 10(b) 3D surface with distributed layer, Ra −0.325 μm, Rt −4.5 μm, and Rt/Ra > 10. Kurtosis 4.39 and skewness 0.058 indicate that the surface comprises a wavy texture mostly centric.

4. Conclusions

(i) A gray cast iron/steel sliding contact pair, with contact pressure of 0.6 MPa to 1.7 MPa, exhibits stick-slip contact wear, which has a predominance of ploughing behavior. Positive as well as a negative wear mode was shown depending on the contact pressure and sliding velocity

(ii) With 40 pride oil, an additive oil, the counter steel pin surface exhibits mostly negative wear, while GCI disc exhibits mostly positive wear, while GCI disc exhibits fluctuating wear with a rise in wear for higher contact speeds. At relatively lower contact pressure and temperature, the effectiveness of oil addition could not be realized

(iii) Micrograph of GCI disc tested with 40 pride oil exhibits +ve mode of wear with the worn-out surface exhibiting surface cracking and discrete pits

(iv) The higher surface roughness values Ra −0.682 μm were obtained at 45 N, 0.5 m/s, 900 m and lower surface roughness values (Ra 0.18 μm) were obtained at 30 N, 1.0 m/s, 900 m

(v) Lubricated sliding results in relatively reduced order of coefficient of friction, attributable to better load distribution due to formation of lubricant film

Data Availability

The data used to support the findings of this study are included within the article.

Conflicts of Interest

The authors declare that they have no conflicts of interest regarding the publication of this paper.

References

[1] R. Evans, *Metalworking Fluids (MWFs) for Cutting and Grinding*, Woodhead Publishing, 2012.

[2] S. Ananth, J. Udaya Prakash, R. Krishna Murthy, K. V. Arun Pillai, and T. V. Moorthy, "Tribological behaviour of grey cast

iron–EN31 steel contact under sliding conditions," *Transactions of the Indian Institute of Metals*, vol. 73, no. 3, pp. 793–798, 2020.

[3] S. Ananth, J. Udaya Prakash, T. V. Moorthy, and P. Hariharan, "Wet sliding wear optimization of gray cast iron using Taguchi technique," *International Journal of Vehicle Structures and Systems*, vol. 7, no. 4, pp. 154–156, 2015.

[4] B. K. Prasad, "Sliding wear response of a cast iron under varying test environments and traversal speed and pressure conditions," *Wear*, vol. 260, no. 11-12, pp. 1333–1341, 2006.

[5] W. Grabon, W. Koszela, P. Pawlus, and S. Ochwat, "Improving tribological behaviour of piston ring-cylinder liner frictional pair by liner surface texturing," *Tribology International*, vol. 61, pp. 102–108, 2013.

[6] S. Kawada, S. Watanabe, C. Tadokoro, R. Tsuboi, and S. Sasaki, "Lubricating mechanism of cyano-based ionic liquids on nascent steel surface," *Tribology International*, vol. 119, pp. 474–480, 2018.

[7] V. Nayyar, J. Kaminski, A. Kinnander, and L. Nyborg, "An experimental investigation of machinability of graphitic cast iron grades; flake, compacted and spheroidal graphite iron in continuous machining operations," *Procedia CIRP*, vol. 1, pp. 488–493, 2012.

[8] G. Straffelini and L. Maines, "The relationship between wear of semimetallic friction materials and pearlitic cast iron in dry sliding," *Wear*, vol. 307, no. 1-2, pp. 75–80, 2013.

[9] E. E. Vera-Cardenas, R. Lewis, and T. Slatter, "Sliding wear study on the valve-seat insert contact," *Open Journal of Applied Sciences*, vol. 7, no. 2, pp. 42–49, 2017.

[10] A. R. Riahi and A. T. Alpas, "Wear map for grey cast iron," *Wear*, vol. 255, no. 1-6, pp. 401–409, 2003.

[11] A. Vadiraj, M. Kamaraj, and V. S. Sreenivasan, "Wear and friction behavior of alloyed gray cast iron with solid lubricants under boundary lubrication," *Tribology International*, vol. 44, no. 10, pp. 1168–1173, 2011.

[12] K. Chawla, N. Saini, and R. Dhiman, "Investigation of tribological behavior of stainless steel 304 and grey cast iron rotating against EN32 steel using pin on disc apparatus," *IOSR Journal of Mechanical and Civil Engineering*, vol. 9, no. 4, pp. 18–22, 2013.

[13] K. Masuda, N. Oguma, M. Ishiguro, Y. Sakamoto, and S. Ishihara, "Sliding wear life and sliding wear mechanism of gray cast iron AISI NO.35B," *Wear*, vol. 474-475, p. 203870, 2021.

[14] M. A. Maleque, S. Shah, and N. N. Razali, "Wear behavior of aluminium modified cast iron in comparison with conventional gray cast iron," in *Reference Module in Materials Science and Materials Engineering*, pp. 1–7, Elsevier, 2018.

[15] H. Singh and H. Bhowmick, "Tribological behaviour of hybrid AMMC sliding against steel and cast iron under MWCNT-oil lubrication," *Tribology International*, vol. 127, pp. 509–519, 2018.

[16] B. K. Prasad, "Sliding wear response of a grey cast iron: effects of some experimental parameters," *Tribology International*, vol. 44, no. 5, pp. 660–667, 2011.

[17] S. Ananth, A. R. Sivanesh, J. Udaya Prakash, and P. John Paul, "Wear parameter optimisation of piston and cylinder liner material (GCI) using Taguchi technique," *International Journal of Ambient Energy*, pp. 1–5, 2019.

[18] P. Sivaprakasam, A. Kirubel, G. Elias, P. Maheandera Prabu, and P. Balasubramani, "Mathematical modeling and analysis of wear behavior of AlTiN coating on titanium alloy (Ti-6Al-4V)," *Advances in Materials Science and Engineering*, vol. 2021, Article ID 1098605, 2021.

[19] P. Sivaprakasam, G. Elias, P. Maheandera Prabu, and P. Balasubramani, "Experimental investigations on wear properties of AlTiN coated 316LVM stainless steel," *Materials Today: Proceedings*, vol. 33, no. 7, pp. 3470–3474, 2020.

[20] S. Abdou and A. Elkaseer, "Wear behaviour of grey cast iron with the presence of copper addition," *Advances in Mechanical Engineering*, vol. 10, no. 10, Article ID 168781401880474, 2018.